Journal of *Marine Science and Engineering*

MDPI

Article

Artificial Electrolytic Structures as Mitigation and Restoration Elements from Environmental Impacts in Marine Habitats

Miguel-Ángel Climent [1,*], Carlos Antón [1,2], Antonio Aldaz [3,†], Alejandro Carmona-Rodríguez [2], Pedro Garcés [1], Vicente Montiel [3], Aitor Forcada [2] and Alfonso A. Ramos-Esplá [2,4]

[1] Department of Civil Engineering, University of Alicante, 03690 Alicante, Spain; c.anton@ua.es (C.A.); pedro.garces@ua.es (P.G.)
[2] Department of Marine Science and Applied Biology, University of Alicante, 03690 Alicante, Spain; alejandro.carmona@ua.es (A.C.-R.); forcada@ua.es (A.F.); alfonso.ramos@ua.es (A.A.R.-E.)
[3] Institute of Electrochemistry, University of Alicante, 03690 Alicante, Spain; vicente.montiel@ua.es (V.M.)
[4] Centro de Investigación Marina de Santa Pola (CIMAR), University of Alicante, 03690 Alicante, Spain
* Correspondence: ma.climent@ua.es
† (Deceased).

Abstract

This work describes a method to create submarine artificial structures based on light metallic structures covered by calcareous layers obtained by electrolysis in sea water, with full environmental safety of the process. For structures based on meshes of cylindrical steel wire, the thickness of the deposited layer increases linearly with time for widths up to 2 mm. In the case of thicker layers, mathematical modelization suggests that the evolution of the deposited layer width might not be linear. Under the experimental conditions of this work, the deposited layers were mainly composed of stable crystalline forms of calcium carbonate. No significant presence of magnesium containing minerals was found in the deposited layers. The composition and texture of the obtained surfaces might be deemed as optimum from the point of view of providing colonization sites for the sessile benthic organisms of interest. These structures may be used as elements that can be included in the design of environmental remediation applications. Regarding their potential applications, once deployed in the marine environment and colonized by sessile benthic filter-feeding species, the structures could contribute to the improvement of sea water quality in commercial ports or marinas, which might be affected by organic pollution.

Keywords: artificial reefs; electrolytic reefs; biofouling; marine eco-engineering

Academic Editor: Huiwang Gao

Received: 31 January 2026
Revised: 26 May 2026
Accepted: 27 June 2026
Published: 30 June 2026

1. Introduction

The degradation of marine habitats can be attributed to numerous factors, among which are marine heatwaves that deepen the seasonal thermocline, illegal fishing activities, degradation caused by organic waste originating from fish fattening cages in industrial aquaculture facilities, organic loads generated by discharges, stagnant waters and overflow outlets, as well as the potential overcrowding of divers. Diverse strategies have been proposed to mitigate these problems. The use of artificial structures deployed in the marine environment might represent a potential solution for some of the abovementioned problems [1].

Among these artificial structures are artificial reefs, which are installed on the seabed for a wide range of purposes—including the enhancement of fisheries through seabed protection, recreational diving, habitat restoration, and coastal defense [2]. Over the past

two decades, research on artificial reefs has evolved from a fisheries-oriented focus toward an approach centered on the rehabilitation and restoration of marine ecosystems and the mitigation of anthropogenic impacts [3]. During this period, there has been a notable shift in the materials employed [4]—from waste or so-called "opportunistic materials," such as tires, scrapped vehicles, ships, and oil platforms, to ad hoc construction materials specifically designed for particular functions (e.g., fishing, seabed protection and rehabilitation, and diving), including concrete, PVC, fiberglass, iron/steel, and other materials. In fact, in the Valencian Community (Spain), concrete artificial reefs have been developed primarily as deterrent elements against trawling [5,6], with the aim of protecting seagrass meadows and calcareous algal beds.

However, the global increase in the deployment of such structures has raised concerns regarding their potential negative impacts [7], particularly in relation to the use of unsuitable materials, which has led to the development of operational guidelines and protocols [8–10]. In this context, an emerging technology known as marine eco-engineering or green marine construction [11] has been developed to minimize the environmental footprint of submerged infrastructures and to promote the use of "eco-friendly materials" [12–16].

Among the new materials being explored are carbonated structures generated by electrolysis on a metallic matrix, originally developed by Hilbertz in the late 1970s [17–20]. It has been known for a long-time that the main cathodic reactions on a metallic surface during electrolysis in sea water are the reduction of dissolved oxygen and the reduction of water molecules leading to the evolution of gaseous hydrogen:

$$\tfrac{1}{2}\,O_2\,(aq) + H_2O + 2\,e^- \rightarrow 2\,OH^-\,(aq) \quad (1)$$

$$2\,H_2O + 2\,e^- \rightarrow H_2\,(g) + 2\,OH^-\,(aq) \quad (2)$$

Both of these reactions give rise to a local increase of pH in the surroundings of the cathodic zones. Hence, due to the composition of sea water, some insoluble compounds, namely calcium carbonate and magnesium hydroxide, can precipitate at the cathodic zones [21]:

$$Ca^{2+}\,(aq) + HCO_3^-\,(aq) + OH^-\,(aq) \rightarrow CaCO_3\,(s) + H_2O \quad (3)$$

$$Mg^{2+}\,(aq) + 2\,OH^-\,(aq) \rightarrow Mg(OH)_2\,(s) \quad (4)$$

The formation of calcareous deposits, a term which is often used to describe magnesium- and calcium-containing compounds, is a feature associated with the protection of steel structures immersed in sea water against corrosion through cathodic protection [22,23]. It is also well known that these calcareous deposits have the beneficial effect of reducing the rate of corrosion of unprotected steel and iron exposed to sea water [24–26]. This effect is also found in cases of microbiologically-induced corrosion of steel in sea water [27].

The electrochemical process for fabricating underwater structures, based on electrolysis in sea water, has been applied in various coastal regions worldwide for the restoration of degraded coral reefs and other applications [28–35]. Nevertheless, to the best of our knowledge, there are no records of its implementation along the Spanish coasts—neither as a tool for biodiversity restoration nor as a biofiltration or impact-mitigation element.

Several patented procedures can be found in the literature that propose the use of electrolysis in seawater for the creation of artificial reefs and other applications, employing direct, pulsed, or intermittent current [18–20,36]. One of the possible drawbacks in the procedure is the potential generation of toxic substances such as chlorine gas, as well as the possible release of heavy metal ions in the case of certain types of anodes. Another patented method [37] describes the possibility of using a galvanic pair system to obtain

a calcareous deposit by electrolysis on an iron or steel cathode—namely, by exploiting the creation of an electrochemical cell through electrical contact between the cathode and an anode made of a metal less noble than steel (such as aluminium, zinc, or magnesium). The possible drawbacks of this system include the lack of control over electrochemical parameters (current intensity and potential difference) and, again, the potential release of heavy metal ions from specific anode materials.

For the reasons outlined above, it would be of interest to develop a system capable of generating carbonated structures through electrolysis in sea water, while being as innocuous as possible without altering the ecosystem it is intended to restore.

The objective of the research project, within which this publication is framed, was to demonstrate the feasibility of a manufacturing system for metallic structures coated with calcareous layers induced by electrolysis. The system aims were to combine minimal disturbance to the marine environment with high flexibility, ease of production and deployment, and overall cost efficiency. These structures may be used by marine biologists and engineers as elements that can be included in the design of environmental remediation applications. Regarding their potential applications, once deployed in the marine environment and colonized by sessile benthic filter-feeding species, the structures could have a positive impact on the improvement of sea water quality in commercial, fishing, and recreational ports, which might be affected by organic pollution. Moreover, the fabrication of structures with biofiltration capacity could be valuable in the aquaculture sector, contributing to the reduction of organic loads associated with fish fattening (e.g., feces and uneaten feed). Likewise, the production of recreational reefs could attract sport divers, enabling the establishment of new diving areas away from environmentally sensitive zones—thereby redirecting interest toward potential underwater parks and reducing pressure on habitats of high biological value. Another important objective was to test the possibility of using renewable energy sources, such as solar photovoltaic systems, for providing the energy needed during the electrolysis step. This possibility is relevant in cases of stand-alone applications in zones without access to the conventional electric energy net, for instance when trying to produce the structures on-site at locations far from the shore.

The study describes the characteristics of the structures that can be obtained through the procedure detailed in a patented utility model developed by the authors and approved by the Spanish Patent and Trademark Office [38,39], with particular emphasis on using solar photovoltaic systems for providing the electric energy needed for the electrolysis. It also presents preliminary information on the nature of the calcareous deposits obtained by electrolysis and the growth rate of the $CaCO_3$ layer thickness. Finally, the innovative component and potential impacts of the proposal are discussed.

The results of our studies on the capacity of calcareous surfaces obtained by electrolysis in sea water to promote sessile benthic species colonization compared to other reference substrates were published previously [40,41].

2. Materials and Methods

The manufacturing process of the electrolytically produced structures in the marine environment was described in detail in previous publications [38,39]. Through this process, lightweight structures are obtained, consisting of a metallic substrate coated with calcareous or calco–magnesian stony layers whose surface texture (porosity and roughness) and hardness are comparable to those of natural marine limestone or to the material excreted by corals.

The device comprises a steel mesh cathode—allowing the use of any commercially available mesh—and a metallic anode. These units (cathode and anode) form the basic electrolytic cell responsible for the formation of the calcareous deposit on the cathode surface. Both the shape and size, as well as the geometric characteristics of the cathode (for example, mesh aperture), can be selected according to the requirements or objectives of the structure. In this work the cathode consisted of an electro-welded mild steel mesh (diameter of the wire 4 mm and square mesh openings of 150 mm) conformed with a cylindrical shape (diameter 50 cm and height 105 cm); see Figure 1a. The anode used was another steel mesh cylinder with larger dimensions and weight than the cathode. It should be considered that a steel anode will progressively corrode in the course of electrolysis. This means that the anode dimensions and mass should be designed to allow the completion of the electrolytic process. Alternatively, the anode can be replaced by a new one in case of exhaustion of the anode with long term electrolytic processes. The use of a steel anode makes the massive release of chlorine gas in electrochemical anodic reactions unlikely.

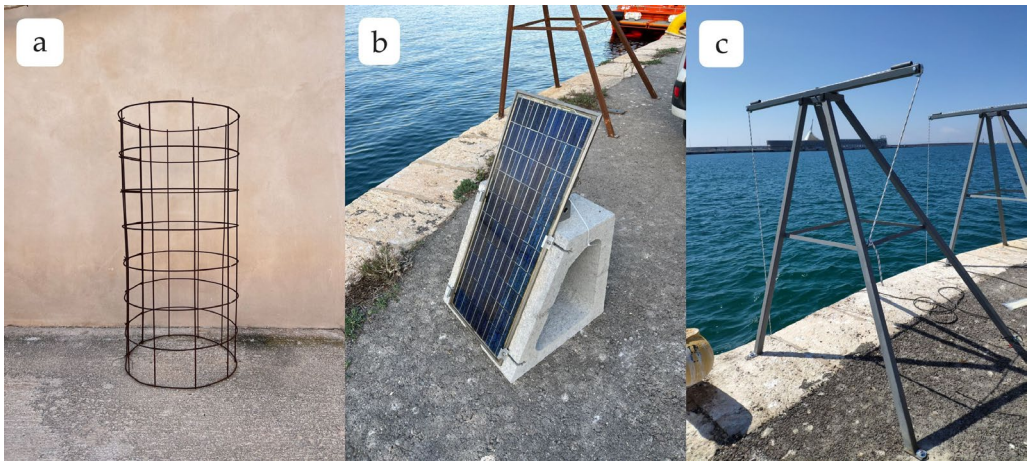

Figure 1. Elements used in the fabrication of the carbonated structures. (**a**) Cathode consisting of an electro-welded mild steel mesh conformed with a cylindrical shape. (**b**) Photovoltaic panel connected to a battery equipped with a current limiting system. (**c**) Disposition of the cranes in one of the docks of the Port of Alicante, Spain. (Photos: C. Antón).

The electrolysis processes were energized by using photovoltaic solar panels. Three tests were performed, termed as A, B, and C. Table 1 contains the most relevant characteristics of these tests. Three photovoltaic solar panels were used with different characteristics, see Table 1. For test A the panel was not connected directly to the electrolytic cell. Instead, the solar panel was connected to an energy storage system (battery), and the battery, equipped with a system for limiting the current intensity at 0.8 A, was the energy source for the electrolysis process. Considering the geometric surface of the cathode, this current intensity is equivalent to an apparent cathodic current density of 1800 mA/m^2 for test A. Unlike, in both tests B and C, the photovoltaic panels were directly connected to the electrolysis cells. Data acquisition systems were used for monitoring the current intensity provided by the solar panel in tests B and C. Hence, test A was performed in galvanostatic conditions (constant current intensity), while tests B and C were run at non-constant current intensities because of the variations of the current outputs of the panels, due for instance to daily variations of the received insolation. Figure 1b shows a photo of one of the photovoltaic panels. The duration of the electrolysis processes was approximately 125 days.

Table 1. Characteristics of the electrolysis tests.

Test	Parameters of the Photovoltaic Panels		Use of Energy Storage (Battery)	Constant Current Intensity (A)
	Maximum Power (W)	Intensity at Max. Power (A)		
A	40	2.0	Yes	0.80
B	20	1.09	No	-
C	5	0.28	No	-

All the tests were performed at Dock number 9 of the Port of Alicante, Spain (38°20′09.23″ N–00°29′05.81″ W), located SE of the Iberian Peninsula. Figure 1c shows the disposition of the cranes used for the immersion and hoisting of the structures, which were submerged at an approximate depth of 1 m from the sea surface. The characteristics of the sea water at the testing site were the following: sea water temperature was 14.9 °C at the beginning and 19.4 °C at the end of the tests; pH and salinity were practically constant at values of 8.09 ± 0.04 and 37.0 ± 0.4 PSU, respectively.

For the purpose of studying the growth process of the electrolytically deposited calcareous layers, the structures were hoisted from the sea at 35, 66, 84, and 124 days from the beginning of the electrolysis. At these times, measurements of the diameter of the steel wires were taken at 10 different points to obtain the mean value of the radius of the coated steel meshes. The ten measurement points were selected using a stratified random-sampling approach to ensure spatial representativeness of the carbonated structure. The cylindrical cathode was divided into ten zones distributed along both the height and the lateral face of the cylinder, covering the lower, middle, and upper zones, as well as different angular orientations. Within each position, the exact measurement point was randomly selected while avoiding areas with visible discontinuities (edges, mesh joints, local deformations of the mesh or material losses) in order to obtain representative thickness values of the carbonated deposit. The thickness of the carbonated layer was measured using a digital caliper (Mitutoyo Digimatic, model CD-6″ ASX, Mitutoyo Corporation, Kawasaki, Japan, resolution 0.01 mm). The reported values correspond to the mean of the ten measurements obtained for each structure.

Furthermore, small samples were taken from the material constituting the coatings at 35 and 66 days from the beginning of the tests, with the aim of studying the mineralogical composition of the coatings through X-ray diffraction (XRD) analysis. Powder samples were obtained from each structure by cutting a fragment of approximately 10 cm from the steel mesh at a randomly selected location. The deposited calcareous layer was mechanically removed by gentle scraping using a spatula until the entire precipitated material from the fragment was collected. The recovered material was then finely ground in an agate mortar to obtain a homogeneous powder suitable for XRD measurement. One representative powder sample was analyzed by XRD for each experimental condition and testing time.

The XRD equipment was a BRUKER, model D8-Advance (Bruker AXS GmbH, Karlsruhe, Germany). The radiation used was Cu $K\alpha_1$ (λ = 1.5406 Å), with a scintillation detector. The total time of data acquisition for the diffractograms was 66 min (2θ range 4–70° with a step-size of 0.05°, i.e., 3 s/point). No base line correction was applied to the diffractograms. Quantitative Rietveld analysis of the obtained diffractograms were performed using the software TOPAS 5.

3. Results

3.1. Evolution of the Deposited Calcareous Layer Thickness

Figure 2 shows the evolution of the mean radius of the steel wires due to growth of the electrolytically deposited calcareous layers for the different tests (each point represents the mean value of ten radius measurements at different locations on the cathodic steel mesh). The study was limited to about 125 days of electrolysis. For test A, the final radius was of about 4 mm (see Figure 2 (A)); i.e., the deposited calcareous layer had a thickness of about 2 mm. For the practical applications of this work a calcareous layer of about 1 to 2 mm was taken as enough. On the other hand, for tests B and C the final thickness of the deposited layer was of about 0.6 mm after 125 days of electrolysis (approximately 4 months). It appears that the use of a constant current system (test A) gives rise to quicker growth (approximately 1 mm in 2 months). Obviously, this expected difference is due to the discontinuous nature of the electrolysis, fed by the photovoltaic panels alone. Figure 3 shows the records of the evolutions of the current intensities delivered by the photovoltaic panels in tests B and C. In the latter Figure 3, the saw teeth shape of the current intensities is apparent (with peak intensities at mid-day and periods of zero current during the night hours) due to the daily variations of the received insolation.

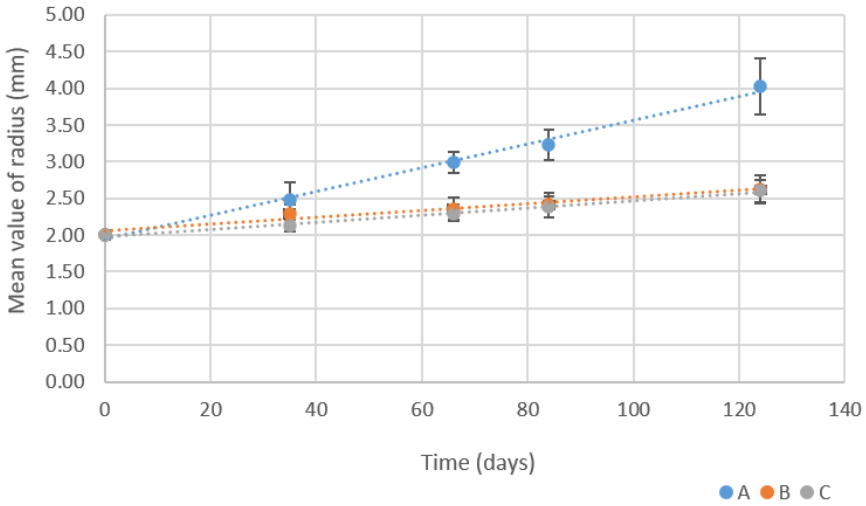

Figure 2. Evolution of the mean radius of the steel wires due to growth of the electrolytically deposited calcareous layers for the different tests; see Table 1. Points: mean values of radius measurements (error bars indicate the standard deviation of the ten measurement sets corresponding to each structure and testing time). Dashed lines: fitted functions obtained in the least-squares linear fittings according to Equation (5).

3.2. Characteristics of the Deposited Calcareous Layers

One of the objectives of this work was to create a new optimal surface for the development of biofouling and colonization by sessile benthic organisms. For this reason, it was necessary to know the composition and texture of the electrolytically-induced deposited layers. To this end small samples, taken from the material constituting the coatings, were subject to XRD analysis, as described in Section 2. Table 2 shows the mineralogical species detected as components of the coatings. The quantification was performed through the Rietveld method, see Section 2. The last two columns of Table 2 give the values of the statistical Rietveld reliability parameters: R_{WP} and GOF (goodness of fit). For the sake of brevity only the diffractograms corresponding to tests A and C (at 66 days) are shown in Figures 4 and 5, respectively.

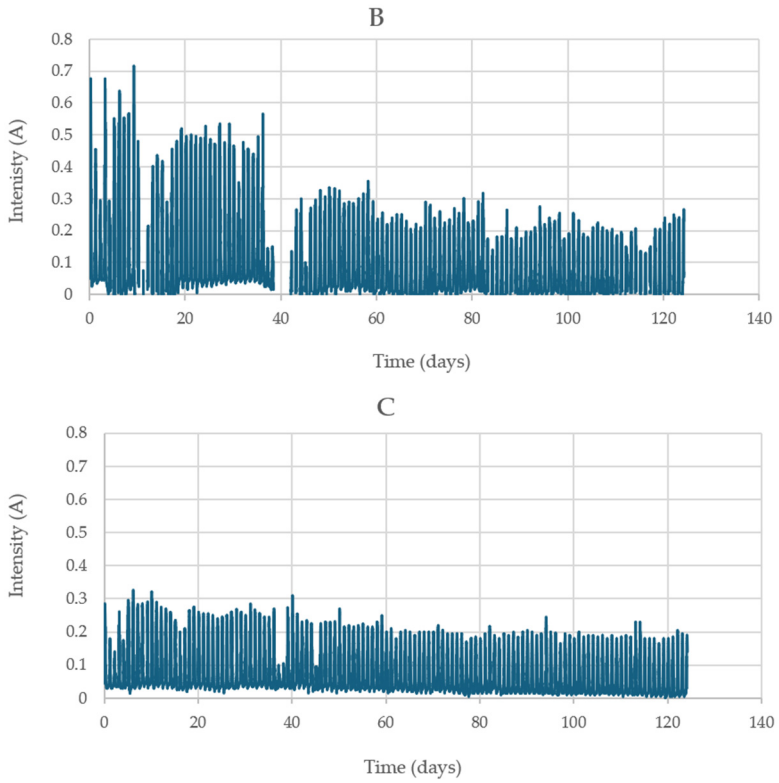

Figure 3. Records of the evolution of the current intensities delivered by the photovoltaic panels in tests B and C.

Table 2. Mineralogical species detected in the X-ray diffractograms as components of the deposited calcareous layers. Component data represent mass percentages in the crystalline phase, calculated through Rietveld analysis, see Section 2.

Test	Time (Days)	Calcite $CaCO_3$	Aragonite $CaCO_3$	Dolomite $CaMg(CO_3)_2$	Quartz SiO_2	Halite NaCl	Albite $Na(AlSi_3O_8)$	R_{WP} (%)	GOF (χ^2)
A	35	14.53	82.04	-	3.43	-	-	9.96	1.14
	66	9.29	90.71	-	-	-	-	10.96	1.24
B	35	45.63	41.90	-	4.13	8.34	-	7.69	1.10
	66	53.35	-	-	8.09	38.56	-	8.62	1.13
C	35	59.79	-	-	29.69	10.52	-	7.15	1.16
	66	51.28	-	12.38	6.60	22.79	6.95	8.88	1.17

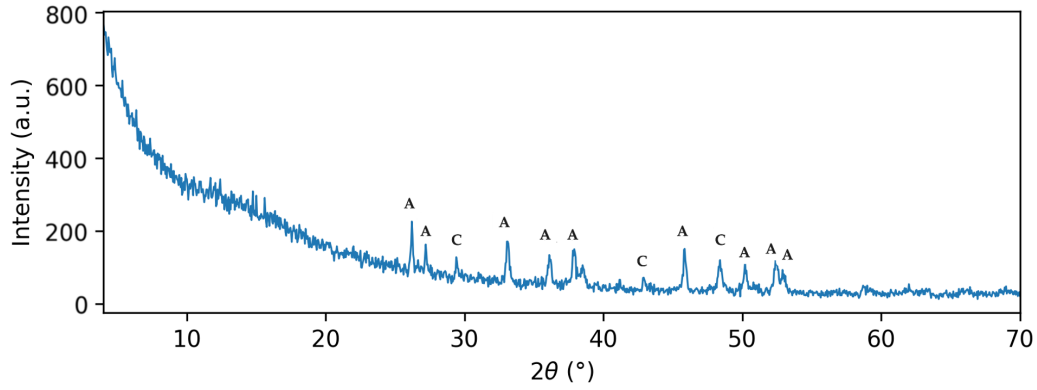

Figure 4. X-ray diffractogram corresponding to the material constituting the calcareous coating in test A at 66 days. A: Aragonite. C: Calcite.

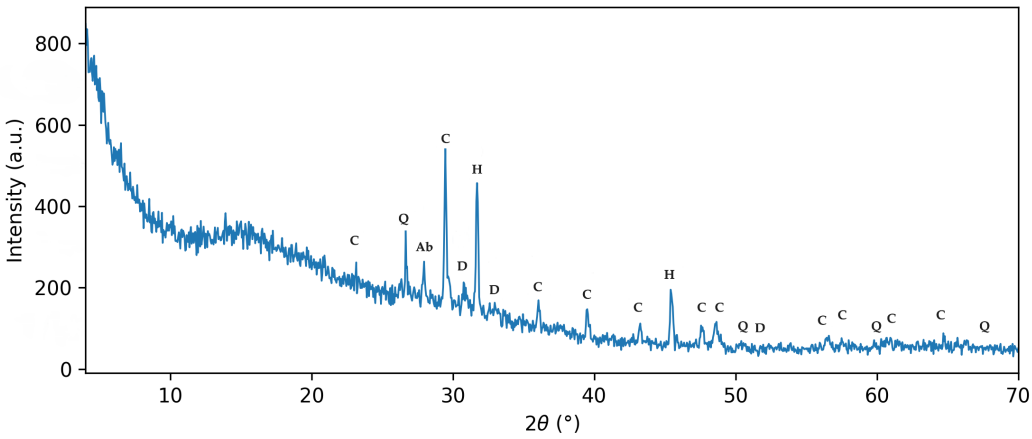

Figure 5. X-ray diffractogram corresponding to the material constituting the calcareous coating in test C at 66 days. C: Calcite. Q: Quartz. D: Dolomite. H: Halite. Ab: Albite.

4. Discussion

4.1. Growth Rate of the Deposited Calcareous Layer Thickness

The evolutions of the mean radius of the steel wire meshes can be described as linear with a good approximation for growths of the calcareous layers up to 2 mm; see Figure 2. These growths can be described by the following equation:

$$r = a\,t + b \tag{5}$$

where r represents the radius of the wire at time t, the slope a represents the radius growth rate (expressed for instance in mm/day), and the intercept b should be approximately equal to the initial radius of the wire (r_0). Table 3 contains the best fit least-squares linear fitting values of Equation (5) to the experimental values of r for the three tests. It is apparent from Table 3 that the growth rate is about 16 μm/day for the constant current test (A), while it is about 5 μm/day for the two tests performed by directly connecting the output of the photovoltaic panel to the electrolysis cell (B and C). The values of the intercept b are very close to 2 mm (initial radius of the steel wire) for the three tests. Furthermore, it seems that for test B the linear fitting is somewhat worse; see the values of the Pearson's correlation coefficient in Table 3. A careful analysis of Figure 2 (B) shows that during the first 35 days the growth rate was higher than later. After the first 35 days, the growth rate seems to be lower. This observation can be related to the variation in peak intensity values shown in Figure 3 (B) after approximately the 35th day. It seems that the efficiency of the photovoltaic panel decreased notably after that day due to some unknown reason. In fact, after the 35th day, the peak intensities of both panels B and C were practically equal, despite panel B having a higher nominal power than panel C; see Table 1. This points to an important aspect to be considered when using photovoltaic panels for stand-alone applications: the efficiency of the energy source might decrease, thus lowering the growth rate and lengthening the duration of the electrolysis process for a predetermined thickness of the deposited calcareous layer.

It was shown that the evolutions of the radius are approximately linear, under the conditions of this work (growth of the calcareous layer thickness of maximum 2 mm); see Figure 2. However, from a theoretical point of view, in the case of growth of a calcareous layer at constant current intensity (constant mass deposition rate) for a cylindrical geometry cathode, the growth rate of the deposited layer should not be constant (non-linear growth); see Appendix A. Most probably this non-linear behavior would be apparent for longer periods of electrolysis, hence a larger thickness of the deposited calcareous layer. Further

research, with longer duration of the electrolysis processes and studying a larger number of replicate samples for each testing condition, should be performed to ascertain the evolution trend of the growth rate of these electrolytic structures in the long term.

Table 3. Best fit least-squares linear fitting parameters of the experimental values of r for the three tests.

Test	a (mm/Day)	b (mm)	Square of Pearson's Correlation Coefficient (ρ^2)
A	0.0162 ± 0.0008	1.940 ± 0.060	0.9927
B	0.0047 ± 0.0006	2.048 ± 0.045	0.9528
C	0.0049 ± 0.0002	1.976 ± 0.018	0.9928

4.2. Characteristics of the Deposited Calcareous Layers and Surface Colonization Capacity by Sessile Benthic Organisms

Regarding the composition of the calcareous layers deposited by electrolysis in sea water, it is appreciated from Table 2 and the diffractograms (Figures 4 and 5) that the main components of the coatings are calcite and aragonite, while other species can be present in some cases, such as dolomite, quartz, halite, and albite. One of the most remarkable aspects of these compositions is the practical absence of magnesium compounds. Sea water contains approximately 1290 mg/L (0.053 M) of Mg^{2+} ion and 412 mg/L (0.010 M) of Ca^{2+} ion. With these ion concentrations it would be expected to find a considerable amount of magnesium compounds, mainly brucite ($Mg(OH)_2$), together with the stable crystalline forms of $CaCO_3$ (mostly calcite and aragonite) in the composition of the calcareous layers; see Equations (3) and (4). Instead, only low intensity peaks corresponding to dolomite ($CaMg(CO_3)_2$) are found in one of the diffractograms; see Table 2 and Figure 5. Many variables have an influence on the nature and composition of the calcareous layers deposited onto metals due to cathodic polarization: electrochemical parameters (electric potential and current intensity), type of metal and state of its surface, composition of the electrolyte, hydrodynamic conditions, presence of biofouling layers on the metal or organic matter in the electrolyte, temperature, etc. [21]. The saturation pH values of the main components of the calcareous layers in sea water are the following: 7.4 for calcite, 7.5 for aragonite and 9.5 for brucite [22]. Natural sea water has an average pH of 8.1 [42]. This means that the $CaCO_3$ (calcite and aragonite) are supersaturated, hence easily precipitated. On the other hand, $Mg(OH)_2$ (brucite) can only precipitate at the interfacial metal–electrolyte zone (where the pH is higher than 9.5). Far away from this zone, the brucite formed meets unfavourable pH conditions, due to the distance from the electrode producing hydroxide ions, and it tends to dissolve [21,31]. This effect would be more intense due to the hydrodynamic conditions of the natural sea exposure. The intense movement of sea water, even within ports, would lead to an immediate mixing and homogenizing action (practical absence of a diffusion layer), thus avoiding the maintenance of high pH conditions at regions not immediately in contact with the metal–electrolyte interface. This would explain the absence of brucite in the composition of the calcareous layers obtained in this work.

It seems that the presence of Mg^{2+} ions tends to favour the formation of aragonite rather than calcite in the calcareous layers obtained by electrolysis in artificial sea water and other calcium and magnesium containing electrolytes [21]. In this work both aragonite and calcite were observed as components of the calcareous layers (Table 2), although it seems that in the tests performed at lower current intensities (test B at 66 days, and test C at 35 and 66 days) only calcite was detected in the X-ray diffraction analysis (Table 2). This points to a possible influence of the electrochemical parameters on the preferred allotropic form of $CaCO_3$ formed, although the low number of tests performed precludes reaching

a clear conclusion of this aspect. More research, studying a larger number of replicate samples for each testing condition, would be necessary on the composition and distribution of the mineralogical components of the calcareous layers obtained by electrolysis in natural sea water exposure.

Figure 6 shows a photo of the calcareous layer surface, immediately after hoisting from the sea water at the end of the electrolysis process. It is an appreciable texture of sufficient roughness and distributed porosity, which might be deemed as optimum from the point of view of providing colonization sites for the sessile benthic organisms of interest.

Figure 6. Appearance of one of the calcareous layers obtained in this work by electrolysis in sea water, immediately after hoisting from sea water. (Photo: C. Antón).

A 12-month ecological succession study was performed by analysing the differences in biofouling assemblages on two different substrates: the electrolytically induced carbonated structures, as described in Section 2, and bare steel structures as a reference. The main results of this research were published previously [40,41]. The study included separate analysis of the biofouling assemblages over the four seasons of the year, from October 2019 to June 2020 [41]. The results showed that the carbonated structures in general presented higher values of species richness, abundance, and complexity, as compared to the control structures (bare steel). Furthermore, the target species, which are the filter feeders (Bryozoa, Bivalvia, and Ascidiacea) were more abundant on the calcareous layers deposited by electrolysis [40]. These results evidenced the potential of the carbonated structures to be used as biofilters.

The capacity of colonization by non-indigenous species (NIS) of both the electrolytically carbonated and bare steel (control) surfaces was also studied in the Port of Alicante [43]. Results showed that most NIS demonstrated a preference for the electrolytically-induced calcareous layers, as compared to the control surface [43]. This pointed to another possible application of electrolytically carbonated structures as elements to be used for the early detection of NIS in port areas.

4.3. Innovative Component and Potential Impacts of the Proposal

The proposed system for fabricating artificial reefs through electrolysis in a saline medium [38] incorporates several innovative elements that collectively distinguish it from conventional artificial reef technologies. First, the method enables the structures to be produced directly at their deployment site or, alternatively, in controlled environments such as swimming pools, port facilities, saltworks, or industrial plants. This operational flexibility allows for stricter process control when required, while also facilitating adaptation to

diverse logistical and environmental conditions. In addition, the system supports a broad range of energy sources for powering the direct current needed for electrolysis, including transformed grid electricity, energy storage systems, and particularly photovoltaic energy. The latter option is especially advantageous for on-site fabrication, as it ensures both energy autonomy and environmental sustainability.

A second innovative aspect lies in the environmental safety of the process. Throughout electrolysis, no toxic or hazardous chemicals are released into the marine environment, nor are any foreign materials introduced apart from the metallic substrate. This substrate becomes coated with a calcareous layer composed primarily of calcium carbonate ($CaCO_3$), whose composition and texture resemble natural limestone or calcareous material produced by corals. Such characteristics significantly enhance the suitability of these structures for biological colonization. The system also offers substantial design flexibility, allowing manipulation of geometric features—such as dimensions, form, and mesh aperture—so that structures can be tailored to functions including biofiltration, biodiversity restoration, or recreational diving enhancement.

Modularity further reinforces the system's innovative character. Lightweight basic units can be easily transported, stored, and assembled into larger, more complex configurations at the deployment site, as illustrated in Figure 7. These include simple cubic or cylindrical forms as well as more "organic" structures derived from assembling smaller components. Due to their low weight, these units require secure anchoring to prevent displacement by marine currents or interactions with activities such as bottom trawling. Their metallic mesh substrate provides a high surface to volume ratio that increases the available area for biofouling attachment, while their low weight also reduces transportation and deployment costs. Beyond these advantages, the system might contribute to carbon sequestration both during the electrolysis stage and later during colonization by calcareous benthic species, thereby reducing the overall carbon footprint. However, the possible contribution to carbon sequestration has not yet been studied and thus needs further dedicated experimental research for its quantification. The calcareous coating also enhances larval settlement of sessile organisms and may serve as a valuable tool in monitoring the presence of non-indigenous sessile marine species.

Overall, the application of this technology for producing underwater structures with calcareous electro-induced coatings has the potential to generate significant positive impacts across multiple sectors—particularly within industrial and port logistics contexts—with implications spanning economic and societal dimensions.

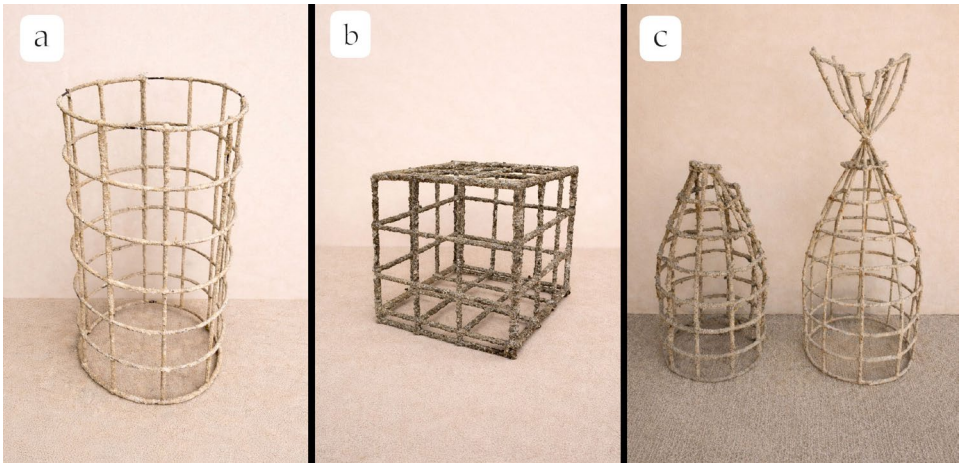

Figure 7. Examples of electrolytically carbonated structures. (**a**) cylinder. (**b**) cube. (**c**) assemblage units for an organic form. (Photos: C. Antón).

4.3.1. Economic Impact

Economically, the proposed system demonstrates a more favourable cost–benefit ratio than many artificial reefs traditionally used in marine habitat restoration, primarily because the structures are lighter than concrete-based alternatives. Their reduced weight simplifies transport both on land and at sea and facilitates efficient deployment operations, which typically represent the costliest phase of reef restoration efforts [6]. The modularity of basic units allows larger structures to be assembled on demand, thereby limiting construction expenditures and reducing transport-related costs.

Furthermore, on site carbonate deposition powered by photovoltaic energy offers an avenue for lowering operational expenses, while also making the system feasible in areas without access to conventional electrical grids. This reliance on renewable energy may additionally stimulate activity and innovation within the clean energy sector. The technology's versatility also opens avenues for new developments in marine eco-engineering and "green marine construction," potentially supporting the creation of new enterprises and associated employment opportunities. Finally, the use of environmentally responsible structures may improve the corporate social responsibility (CSR) standing of ports and private companies, indirectly enhancing their economic performance.

4.3.2. Social Impact

From a social perspective, the system offers several advantages linked to its reliance on non-polluting materials. The structures consist of benign components—steel and seawater derived calcium carbonate—thus providing a more environmentally friendly alternative to opportunistic reefs or concrete structures. Their presence might also contribute to mitigating environmental impacts by helping improve the quality of sea water at marine zones with the presence of organic pollutant loads originating from sources such as aquaculture cages or submarine outfalls. These effects are due to the activity of benthic filter feeding invertebrates that colonize them.

Additionally, the carbonated structures can promote the recovery of degraded habitats by facilitating the settlement of local flora and fauna, thereby enhancing biodiversity and increasing the availability of living marine resources. The establishment of dedicated recreational diving sites can further alleviate pressure on natural ecosystems within protected areas by reducing physical damage caused by direct human activity. Social acceptance of this technology is high, not only because of its non-polluting nature and its capacity to contribute to improvement of sea water quality but also due to its possible contribution to carbon sequestration through the incorporation of carbonate into calcareous layers and skeletal structures of benthic invertebrates—such as anthozoans, serpulids, cirripeds, bivalves, and bryozoans. The integration of renewable energy, particularly photovoltaic systems, further reinforces its environmental and social sustainability [44,45].

5. Conclusions

The work describes a method to create submarine artificial structures based on light metallic structures covered by calcareous layers obtained by electrolysis in sea water, with full environmental safety of the process. Throughout the electrolysis, neither toxic or hazardous substances are released into the marine environment nor are foreign materials introduced apart from the metallic substrate. Other appealing characteristics of the system are as follows: the high operation flexibility regarding the possibility of fabrication on-site or at controlled industrial facilities; the size and shape of the structures; and the possibility of modular construction by assemblage of small elements to obtain big complex structures. The low weight of the structures, as compared to other artificial reefs, simplifies and

reduces the costs of transport and the sea deployment steps. Finally, the electrolysis can be energized with renewable sources like photovoltaic systems.

For metallic structures based on meshes of cylindrical steel wire, the thickness of the deposited calcareous layer increases linearly with time, for widths of the layer up to 2 mm. However, in the case of thicker layers, mathematical modelization suggests that the evolution of the deposited layer width may not be linear. In the experimental conditions of this work calcareous layers of widths between 1 to 2 mm can be obtained in about four months, although in cases of use of photovoltaic systems without energy storage facility, the process might involve longer times.

In the experimental conditions of this work, the deposited calcareous layers were found to be mainly composed of stable crystalline forms of calcium carbonate, namely aragonite and/or calcite. No significant presence of brucite or other magnesium containing minerals was found in the deposited layers. The composition and texture of the obtained surfaces might be deemed as optimum from the point of view of providing colonization sites for the sessile benthic organisms of interest.

6. Patents

The technology and know-how developed in the research project, within which this publication is framed, led to a patented utility model approved by the Spanish Patent and Trademark Office [38].

Author Contributions: Conceptualization, M.-Á.C., A.A. and A.A.R.-E.; methodology, M.-Á.C., C.A., A.C.-R., P.G., V.M., A.F. and A.A.R.-E.; validation, M.-Á.C., P.G., V.M., A.F. and A.A.R.-E.; formal analysis, M.-Á.C., P.G., V.M. and A.A.R.-E.; investigation, M.-Á.C., C.A., A.C.-R., P.G., V.M., A.F. and A.A.R.-E.; resources, M.-Á.C., P.G., V.M. and A.A.R.-E.; data curation, C.A. and A.C.-R.; writing—original draft preparation, M.-Á.C.; writing—review and editing, M.-Á.C., C.A., A.F. and A.A.R.-E.; supervision, M.-Á.C. and A.A.R.-E.; project administration, M.-Á.C. and A.A.R.-E.; funding acquisition, M.-Á.C. and A.A.R.-E. All authors have read and agreed to the published version of the manuscript.

Funding: This study forms part of the ThinkInAzul programme and was supported by MICIU (Spanish Ministry for Innovation, Science and Universities) with funding from the European Union NextGenerationEU (PRTR-C17.I1) and by Generalitat Valenciana (GVA-THINKINAZUL/2021/014; Principal Investigators: A.A. Ramos-Esplá and M.A. Climent, University of Alicante, Spain).

Data Availability Statement: The original contributions presented in the study are included in the article, further inquiries can be directed to the corresponding author.

Acknowledgments: The invaluable collaboration of the Alicante Port Authority, materialized in the temporary permit for the use of spaces and in the support received from its staff, is expressly acknowledged. The authors also thank Servando Chinchón-Payá (Institute of Construction Science Eduardo Torroja—CSIC, Spain) for his help with the quantitative Rietveld analysis of the X-ray diffractograms. The work is dedicated to the memory of the late Antonio Aldaz (who passed away in 2015), from whom the idea came to undertake this research project. We would like to acknowledge also the collaboration of the late Estanislao (Tanis) Viqueira (who passed away in 2014) in the precursor laboratory experiments of the research. During the preparation of this manuscript, the authors used ChatGPT (GPT-5.2, OpenAI)ChatGPT for the purpose of translation of some paragraphs from Spanish into English. The authors have reviewed and edited the output and take full responsibility for the content of this publication.

Conflicts of Interest: The authors declare no conflicts of interest. The funders had no role in the design of the study; in the collection, analyses, or interpretation of data; in the writing of the manuscript; or in the decision to publish the results.

Appendix A. Theoretical Description of the Radius Growth for a Constant Rate Electrodeposition for a Cylindrical Geometry

Figure A1 depicts the main geometric parameters describing the growth of an electrodeposited layer on a metallic electrode with cylindrical shape. Hence, it can describe the growth of the calcareous layer on the cathode (steel wire of length L and circular cross section with initial radius r_0), when performing the electrolysis in sea water. After a time of electrolysis t the radius of the coated cathode is r.

Considering that the deposited material is produced at a constant rate K_1, the deposited mass m after an electrolysis time t can be expressed as follows:

$$m = K_1\, t \tag{A1}$$

$$m = \pi \left(r^2 - r_0^2\right) L\, d \tag{A2}$$

where (d) d stands for the density of the deposited material. By equating expressions A1 and A2 the growth rate of r can be expressed as follows:

$$r = \sqrt{(K_2\, t + r_0^2)} \tag{A3}$$

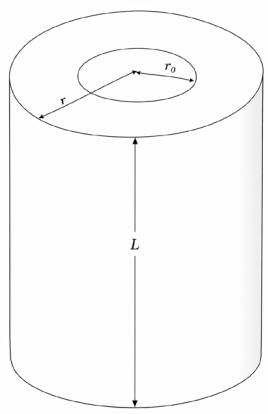

Figure A1. Geometric scheme of the radius growth of a cylindrical shape cathode due to deposition of material as a consequence of the electrochemical reaction:

$$K_2 = K_1/(\pi\, L\, d) \tag{A4}$$

From Equation (A3) the derivative of r with t is the following:

$$\frac{dr}{dt} = \frac{K_2}{2\sqrt{K_2\, t + r_0^2}} = \frac{K_2}{2\, r} \tag{A5}$$

By adopting an arbitrary value of 2 mm^2/day for the constant K_2, which corresponds to a value of K_1 = 17 g/day, for a length of wire of 1 m (1000 mm) and considering a density of the deposited material equal to 2.71 g/cm^3 (value of solid calcite). In these conditions the theoretical growth rate of r, for a wire of initial radius r_0 = 2 mm, is expressed as below:

$$r = \sqrt{(2\, t + 4)} \tag{A6}$$

where r is expressed in mm, and t is expressed in days. Figure A2 shows that the radius growth, according to Equation (A6), can be approximately considered as linear with the time for a short duration of the electrolytically mediated deposition, up to values of 2 mm thickness of the deposited layer; see Figure A2a. On the other hand, for longer term

applications the non-linear character of the radius growth law should be apparent; see Figure A2b.

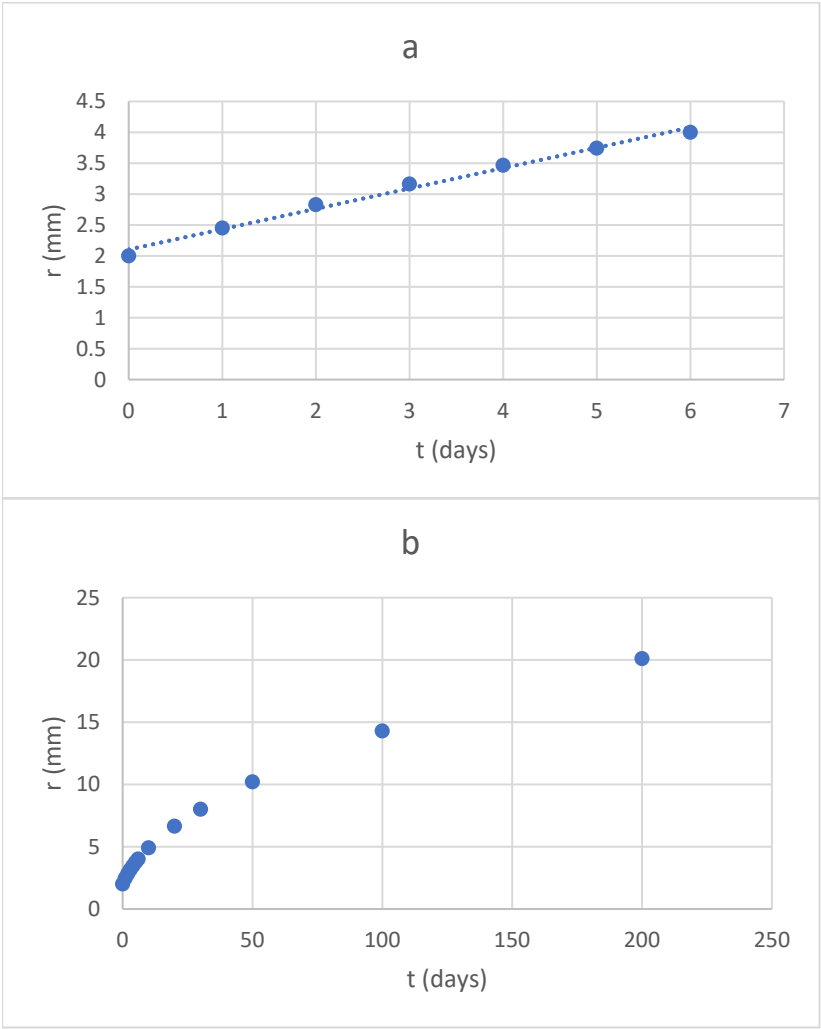

Figure A2. Theoretical growth evolution of the radius of a cylindrical shape electrode due to deposition of material at constant rate, following Equation (A6). (**a**) Radius growth up to 2 mm thickness of the deposited layer. (**b**) Radius growth up to 18 mm thickness of the deposited layer.

References

1. Firth, L.; Knights, A.M.; Bridger, D.; Evans, A.J.; Mieszkowska, N.; Moore, P.J.; O'Connor, N.E.; Sheehan, E.V.; Thompson, R.C.; Hawkins, S.J. Ocean sprawl: Challenges and opportunities for biodiversity management in a changing world. *Oceanogr. Mar. Biol. Annu. Rev.* **2016**, *54*, 189–262.
2. Lee, M.O.; Otake, S.; Kim, J.K. Transition of artificial reefs (ARs) research and its prospects. *Ocean Coast. Manag.* **2018**, *154*, 55–65. [CrossRef]
3. Bayraktarov, E.; Brisbane, S.; Hagger, V.; Smith, C.S.; Wilson, K.A.; Lovelock, C.E.; Gillies, C.; Steven, A.D.L.; Saunders, M.I. Priorities and motivations of marine coastal restoration research. *Front. Mar. Sci.* **2020**, *7*, 484. [CrossRef]
4. Baine, M. Artificial reefs: A review of their design, application, management and performance. *Ocean Coast. Manag.* **2001**, *44*, 241–259. [CrossRef]
5. Belda, L.; Jover, M. *Los Arrecifes Artificiales de la Comunidad Valenciana (The Artificial Reefs of the Valencian Community)*; Consellería de Agricultura y Pesca (Generalitat Valenciana): Valencia, Spain, 1992. (In Spanish)
6. Ramos-Esplá, A.A.; Guillén, J.E.; Bayle, J.T.; Sánchez-Jérez, P. *Artificial Anti-Trawling Reefs Off Alicante, South-Eastern Iberian Peninsula: Evolution of Reef Block and Set Designs*; Jensen, A.C., Collins, K.J., Lockwood, A.P.M., Eds.; Artificial Reefs in European Seas; Springer: Dordrecht, The Netherlands, 2000; pp. 195–218. [CrossRef]
7. Hunter, W. Artificial reefs: A review and critical perspective. *Glasg. Nat.* **2006**, *24*, 39–47.

8. Ministerio de Medio Ambiente. *Guía Metodológica Para la Instalación de Arrecifes Artificiales (Guidelines on Methodologies for Installation of Artificial Reefs)*; Secretaría General Técnica, Ministerio de Medio Ambiente: Madrid, Spain, 2008. (In Spanish)
9. OSPAR. *Guidelines on Artificial Reefs in Relation to Living Marine Resources*; OSPAR Commission Agreement 2013-03 (Reference number: 2012-3); OSPAR: London, UK, 2013.
10. UNEP (United Nations Environment Programme). Updated Guidelines Regulating the Placement of Artificial Reefs at Sea. In Proceedings of the 21st Meeting of the Contracting Parties to the Convention for the Protection of the Marine Environment and the Coastal Region of the Mediterranean and Its Protocols, Naples, Italy, 2–5 December 2019.
11. Dafforn, K.; Glasby, T.; Airoldi, L.; Rivero, N.K.; Mayer-Pinto, M.; Johnston, E.L. Marine urbanization: An ecological framework for designing multifunctional artificial structures. *Front. Ecol. Environ.* **2015**, *13*, 82–90. [CrossRef]
12. Dennis, H.D.; Evans, A.J.; Banner, A.J.; Moore, P.J. Reefcrete: Reducing the environmental footprint of concretes for eco-engineering marine structures. *Ecol. Eng.* **2018**, *120*, 668–678. [CrossRef]
13. Corbau, C.; Nardin, W.; Vaccaro, C.; Vona, I.; Simeoni, U. Experimental design and field deployment of an artificial bio-reef produced by mollusc shell recycling. *Mar. Environ. Res.* **2023**, *183*, 105833. [CrossRef] [PubMed]
14. Cimini, J.; Meroni, L.; Chiantore, M.; Albicini, P.; Pezzilli, C.; Melis, F.; García-Durán, M.; Busquier, L.; Khanuja, J.; Rossi, S.; et al. Addressing challenges in marine algal restoration: Lessons learned from 3D-printed structures on artificial reefs. *Ecol. Eng.* **2026**, *224*, 107885. [CrossRef]
15. ECOncrete Initiative. Available online: https://econcretetech.com (accessed on 9 March 2026).
16. Reef Ball Initiative. Available online: https://reefballfoundation.org (accessed on 13 March 2026).
17. Hilbertz, W.H. Electrodeposition of minerals in sea water: Experiments and applications. *IEEE J. Ocean. Eng.* **1979**, *4*, 94–113. [CrossRef]
18. Hilbertz, W.H. Mineral Accretion of Large Surface Structures, Building Components and Elements. U.S. Patent No. 4246075, 20 January 1981.
19. Hilbertz, W.H. Repair of Reinforced Concrete Structures by Mineral Accretion. U.S. Patent No. 4440605, 3 April 1984.
20. Hilbertz, W.H.; Goreau, T.J. Method of Enhancing the Growth of Aquatic Organisms, and Structures Created Thereby. U.S. Patent No. 5543034A, 6 August 1996.
21. Carré, C.; Zanibellato, A.; Jeannin, M.; Sabot, R.; Gunkel-Grillon, P.; Serres, A. Electrochemical calcareous deposition in seawater. A review. *Environ. Chem. Lett.* **2020**, *18*, 1193–1208. [CrossRef]
22. Neville, A.; Morizot, A.P. Calcareous scales formed by cathodic protection—An assessment of characteristics and kinetics. *J. Cryst. Growth* **2002**, *243*, 490–502. [CrossRef]
23. Hartt, W. 2012 Frank Newman Speller Award: Cathodic protection of offshore structures—History and current status. *Corrosion* **2012**, *68*, 1063–1075. [CrossRef]
24. LaQue, F.J. *Marine Corrosion*; Wiley: New York, NY, USA, 1975.
25. Zhang, J.; Yu, Z.; Zhao, X.; Lan, X.; Wang, J.; Lv, X.; Zhang, C.; Duan, J.; Hou, B. The interaction of biofoulants and calcareous deposits on corrosion performance of Q235 in seawater. *Materials* **2020**, *13*, 850. [CrossRef] [PubMed]
26. Paluzzi, A.; Swain, G.; DeFrancisci, J.; Kuchma, D.; Hansel, C.M. Effects of perforations on internal cathodic protection and recruitment of marine organisms to steel pipes. *J. Mar. Sci. Eng.* **2024**, *12*, 1299. [CrossRef]
27. Melchers, R.E. Long-term marine corrosion under the influence of microbiologically influenced corrosion and calcareous conditions. *Corros. Mater. Degrad.* **2025**, *6*, 46. [CrossRef]
28. Schuhmacher, H.; Schillak, L. Integrated electrochemical and biogenic deposition of hard material–A nature-like colonization substrate. *Bull. Mar. Sci.* **1994**, *55*, 672–679.
29. Siboni, N.; Martínez, S.; Abelson, A.; Sivan, A.; Kushmaro, A. Conditioning film and initial biofilm formation on electrochemical $CaCO_3$ deposition on a metallic net in the marine environment. *Biofouling* **2009**, *25*, 675–683. [CrossRef] [PubMed]
30. Strömberg, S.M.; Lundälv, T.; Goreau, T.J. Suitability of mineral accretion as a rehabilitation method for cold-water coral reefs. *J. Exp. Mar. Biol. Ecol.* **2010**, *395*, 153–161. [CrossRef]
31. Goreau, T.J. *Marine Electrolysis for Building Materials and Environmental Restoration*; Linkov, V., Kleperis, J., Eds.; Electrolysis (cap. 13); IntechOpen: Rijeka, Croatia, 2012. [CrossRef] [PubMed]
32. Goreau, T.J. Electrical stimulation greatly increases settlement, growth, survival, and stress resistance of marine organisms. *Nat. Resour.* **2014**, *5*, 527–537. [CrossRef]
33. Goreau, T.J.; Prong, P. Biorock electric reefs grow back severely eroded beaches in months. *J. Mar. Sci. Eng.* **2017**, *5*, 48. [CrossRef]
34. Margheritini, L.; Colaleo, G.; Contestabile, P.; Larsen-Bjørgård, T.; Enggrob-Simonsen, M.; Lanfredi, C.; Dell'Anno, A.; Vicinanza, D. Development of an eco-sustainable solution for the second life of decommissioned oil and gas platforms: The mineral accretion technology. *Sustainability* **2020**, *12*, 3742. [CrossRef]
35. Mineral Accretion Technology Initiative. Available online: https://oceangardener.org/blog/our-mineral-accretion-technology-test-pilot/ (accessed on 13 March 2026).

36. Benaissa, B.; Verjat, N.; Lansard, M. System and Process for in Situ Electrochemical Treatment, for Capturing Pollutants, Sedimentation and Cleanup of Contaminated Marine Sites. U.S. Patent No. 10414675 B2, 17 September 2019.
37. Streichenberger, A.O. Process for Orienting and Accelerating the Formation of Concretions in a Marine Environment. U.S. Patent No. 4623433, 18 November 1986.
38. Antón, C.; Carmona-Rodríguez, A.; Climent, M.Á.; Garcés, P.; Montiel, V.; Ramos-Esplá, A.Á. Sistema para la Formación de Arrecifes Marinos Artificiales y Estructuras Submarinas con Recubrimiento Calcáreo Inducido por Electrólisis (System for the Formation of Artificial Marine Reefs and Submarine Structures with Calcareous Coating Induced by Electrolysis). Patent No. ES 1278154 Y, 24 September 2021.
39. Antón, C.; Carmona, A.; Climent, M.A.; Garcés, P.; Montiel, V.; Ramos-Esplá, A.A. Sistema para la formación de arrecifes marinos artificiales y estructuras submarinas con recubrimiento calcáreo inducido por electrólisis (Sytem for the formation of articial marine reefs and submarine structures with calcareous coating induced by electrolysis). *Ing. Civ.* **2024**, *203*, 33–42. (In Spanish)
40. Carmona-Rodríguez, A.; Antón, C.; Climent, M.Á.; Garcés, P.; Montiel, V.; Ramos-Esplá, A.Á. Early colonization of sessile megabenthos on electrolytic carbonated structures (Alicante's harbor, Western Mediterranean). *Sci. Total Environ.* **2023**, *900*, 165796. [CrossRef] [PubMed]
41. Carmona-Rodríguez, A.; Antón, C.; Climent, M.-Á.; Garcés, P.; Montiel, V.; Ramos-Esplá, A.A. Sessile biofouling on electrolytic carbonated structures: Stages of colonization and succession. *J. Mar. Sci. Eng.* **2024**, *12*, 443. [CrossRef]
42. Millero, F.J. *Chemical Oceanography*, 4th ed.; CRC Press/Taylor and Francis: Boca Raton, FL, USA, 2013; Chapter 2.
43. Carmona-Rodríguez, A.; Antón, C.; Climent, M.-Á.; Garcés, P.; Montiel, V.; Arroyo-Martínez, E.; Ramos-Esplá, A.A. Development and Succession of Non-Indigenous and Cryptogenic Species over Two Different Substrates in the Port of Alicante (Western Mediterranean). *J. Mar. Sci. Eng.* **2024**, *12*, 1188. [CrossRef]
44. Strain, E.M.A.; Alexander, K.A.; Kienker, S.; Morris, R.; Jarvis, R.; Coleman, R.; Bollard, B.; Firth, L.B.; Knights, A.M.; Grabowski, J.H.; et al. Urban blue: A global analysis of the factors shaping people's perceptions of the marine environment and ecological engineering in harbours. *Sci. Total Environ.* **2019**, *658*, 1293–1305. [CrossRef] [PubMed]
45. Mayer-Pinto, M.; Johnston, E.L.; Bugnot, A.B.; Glasby, T.M.; Airoldi, L.; Mitchell, A.; Dafforn, K.A. Building 'blue': An eco-engineering framework for foreshore developments. *J. Environ. Manag.* **2017**, *189*, 109–114. [CrossRef] [PubMed]